Thin Film Nanostructures Prepared via Self-Assembly of Partly Labile Protected Block Copolymers for Hybrid Patterning Strategies

M. Messerschmidt,[†] M. Millaruelo,[‡] R. Choinska,[§] D. Jehnichen,[†] and B. Voit*,[†]

Leibniz-Institut für Polymerforschung Dresden e.V., Hohe Strasse, 6, D-01069, Dresden Germany; Bayer Material Science AG, BMS-CD-NB-CC, D-51368 Leverkusen, Germany; and Instytut Biotechnologii Przemysłu Rolno-Spozywczego, ul. Rakowiecka 36, 02-532 Warszawa, Poland

Received September 1, 2008; Revised Manuscript Received November 10, 2008

ABSTRACT: Thin nanostructured block copolymer films were prepared using dilute solutions of partly *tert*-butoxycarbonyl (BOC)- and *tert*-butyl (TBU)-protected block copolymers based on 4-hydroxystyrene with varying block ratios. AFM measurements showed different nanostructures and morphologies of the films dependent on the block composition of the employed block copolymers. The nanostructure observed in thin films was compared to that of the bulk samples which was analyzed in detail by temperature-dependent SAXS measurements. In order to improve the regularity of the nanostructures of the as-prepared films, different film preparation techniques, film preparation parameters, and solvents were applied, and their impact on the film morphology was investigated. A complete removal of the BOC protecting groups in a block copolymer film was achieved by heating of a film at 190 °C. This process gave rise to the transformation of a partly BOC-protected block copolymer into the homopolymer poly(4-hydroxystyrene), and thus a switching of the thin film morphology occurred which was investigated by AFM, FI-IR, ellipsometry, and contact angle measurements.

Introduction

Self-assembled systems have attracted much attention since they are considered to be promising alternatives to lithographic techniques for the fabrication of nanoscopic devices.[1] In this respect block copolymers are very promising candidates as they frequently segregate into defined periodic structures with dimensions in the range between 10 and 100 nm.[2] The size of these structures (microdomains) is mainly governed by the molar masses of the blocks while the type of the nanostructure (morphology) is controlled by their volume fractions. Typically, the morphology in bulk can be lamellar, gyroid, cylindrical, or spherical.[3,4] When block copolymers are used for the preparation of thin films, additional factors come into play. Krausch et al. reported fundamental studies in which is shown that the morphologies of block copolymers in thin films are governed by the interplay of the surface field and the film thickness.[5,6] Deviations in morphology from that of the bulk structure have been observed like a wetting layer, cylinders with necks, perforated lamellae, and more complicated structures.[7] Because of a preferential wetting of one block at an interface, a parallel alignment of the domains with respect to the substrate is induced and can go through the entire film. For many practical applications, however, a vertical orientation of the microdomains in the polymer film as well as a high regularity of ordered structures over large areas is absolutely necessary. A perpendicular orientation of the microdomains can be achieved by the use of electrical fields[8−11] or by employing neutral surfaces.[12,13] Solvent evaporation at a controlled rate is also a strong highly directing field which can be used for a perpendicular orientation of the microdomains.[14] Russell et al. showed that a controlled solvent evaporation combined with solvent annealing is a robust method to create highly oriented and nearly defect-free nanostructures over large film areas.[15−18] Topographic patterns with nanostructured geometry (graphoepitaxy) can also assist the formation of regular self-assembled microdomains in block copolymer films, providing high orientation and nearly perfect epitaxial long-range order.[19−24] Since the needed topographic patterns are normally prepared by means of photolithography, graphoepitaxy is a very good example that shows the synergy of combining traditional top-down with new bottom-up patterning techniques.[25] Another important strategy for a perpendicular orientation of the microdomains is the use of chemically nanostructured substrates.[26−29] The chemically prestructured patterns used for this method are prepared by means of extreme ultraviolet interferometric lithography (EUV-IL), another example for a successful hybrid patterning approach. Moreover, photolithography has also been applied for direct chemical modification reactions in the microdomains of the self-assembled block copolymer films. For producing nanoporous cross-linked templates, self-assembled PS−PMMA block copolymer films with vertically oriented cylindrical PMMA microdomains were prepared. Exposure with UV light leads to a cross-linking of the PS matrix (major component), whereas the PMMA domains were completely photodegradated and could be removed by a washing procedure.[9,30,31] Ober et al. have also used an asymmetric poly(α-methylstyrene-*block*-4-hydroxystyrene) block copolymer for the preparation of a self-assembled thin film with a cylindrical morphology.[32] In the prepared thin films also small amounts of TMMU and a photoacid generator are distributed. Upon exposure with low levels of UV light the photoacid generator triggers the generation of acid that catalyzes selectively the reaction of TMMU with the hydroxy groups to cross-link the poly(4-hydroxystyrene) blocks in the film matrix. A further exposure with high levels of UV light in a vacuum gives rise to a full degradation and a removal of the cylindrical microdomains with the poly(α-methylstyrene blocks) to form empty pores. By the use of a photolithographic mask, this process can be selectively performed in laterally defined areas of the polymer films, enabling the formation of a hierarchical structure in thin films from the macroscale down to the nanoscale.

When partly photo- or thermolabile protected block copolymers are used as materials for the preparation of self-assembled nanostructured thin films, the scope of flexibility and utility of such systems can be further strongly expanded. A promising block copolymer to this end is a partly BOC- or TBU-protected

* To whom correspondence should be addressed: fax +49 351 4658565; e-mail voit@ipfdd.de.
[†] Leibniz-Institut für Polymerforschung Dresden e.V.
[‡] Bayer Material Science AG.
[§] Instytut Biotechnologii Przemysłu Rolno-Spozywczego.

10.1021/ma8019915 CCC: $40.75
Published on Web 12/12/2008

Table 1. Expected Morphologies of the Used Partly BOC- and TBU-Protected Block Copolymers with Varying Block Ratios and Molar Masses

partly protected block copolymer	$M_{n,cal}$ [g/mol][a] unprotected block	$M_{n,cal}$ [g/mol][a] protected block	$M_{n,cal}$ [g/mol][a](total)	molar mass ratio of the blocks (by NMR)[a]	expected morphology
P(H-OSt-*b*-BOC-OSt) 1:9 (**26**)	6 100	54 600	60 700	1:9	spherical
P(H-OSt-*b*-BOC-OSt)1:5 (**27**)	6 900	32 800	39 700	1:4.7	spherical/cylindrical
P(H-OSt-*b*-BOC-OSt) 1:3 (**28**)	6 900	20 700	27 600	1:3	cylindrical
P(BOC-OSt-*b*-H-OSt) 1:1 (**29**)	14 600	16 100	30 700	1:1.1	lamellar
P(TBU-OSt-*b*-H-OSt) 1:1 (**19**)	22 800	23 100	45 900	1:1	lamellar
P(H-OSt-*b*-TBU-OSt) 1:9 (**30**)	6 100	59 900	66 000	1:9.8	spherical

[a] Details on molar mass determination, calculation of the theoretical molar masses, and the structural characterization have been presented previously.[37]

block copolymer based on 4-hydroxystyrene, since these protecting groups can be selectively removed by a photolithographic induced process leading to poly(4-hydroxystyrene) homopolymer.[33−36] Consequently, when a nanostructured thin film is prepared with such a partly protected block copolymer, a transformation of the block copolymer into a homopolymer leads also to a switching of the film morphology. By applying a photolithographic mask, just the exposed areas of a nanostructured thin film should be selectively transformed. This approach could therefore be used to create laterally defined areas containing a homogeneous film and compartments still bearing the self-assembled nanostructured film. The phenolic OH group in the different film areas is also a versatile functionalizable group which offers great potential for further film modification reactions.

In our previous work we reported on the synthesis of suitable BOC- and TBU-protected block copolymers prepared by nitroxide-mediated radical polymerization.[37] In this work we will now report on the preparation of nanostructured thin films from those block copolymers and the factors which influence the observed microdomain structure and their regularity, an important step on the way to explore hybrid patterning.

Experimental Section

Materials. The employed block copolymers were previously synthesized as reported,[37] and their characteristics are listed in Table 1. Highly polished silicon wafers containing a layer of 50 nm silicon dioxide were purchased from the Institute of Semiconductors and Microsystems Techniques at the Technical University of Dresden. Diglyme (Aldrich, 99%), dioxane (Acros Organics, >99.5%), dichloromethane (Merck, ≥99.8%), ammonia hydroxide (Acros Organics, 28−30 wt % NH_3 in water), and H_2O_2 (Merck, ≥30%) were used as received.

Thin Film Sample Preparation. Highly polished silicon wafers were first precleaned in an ultrasonic bath for 15 min using dichloromethane as solvent. Then, they were treated with a cleaning solution consisting of ammonia hydroxide, H_2O_2, and water (1:1:1 by volume) at 70 °C for 60 min. Finally, the wafers were thoroughly rinsed with Millipore water and dried in a nitrogen flow.

For the film preparation by dip-coating a homemade device fabricated at the Leibniz Institute of Polymer Research Dresden was applied.[38] Dip-coating was performed with freshly cleaned silicon wafers and with filtered polymer solutions of 1 wt % (filter size: 0.2 μm) using diglyme or dioxane as solvent. Film formation occurred in a hermetic closed chamber (desiccator) with an atmosphere strongly enriched with solvent vapor. The withdrawal rates were either 1.8 or 11.3 cm/min.

Film preparation via spin-coating was performed with a filtered (filter pores: 0.2 μm) 2 wt % polymer solution with diglyme as solvent and freshly cleaned silicon wafers on a "Photo Resist Spinner" of Headway (Headway Research Inc., Garland, TX) under normal conditions.

Instrumentation. AFM measurements were performed on a Dimension 3100 NanoscopeIV from Digital Instruments Inc. (Santa Barbara, CA) in the tapping mode. Phase and height images were recorded simultaneously with a value of r_{sp} (A_{sp}/A_0) in the range between 0.6 and 0.7 ("moderate tapping") in order to ensure that the interactions between the tip and the film surface is repulsive in nature. Under these settings the contrast of the phase image is directly correlated with the viscoelastic behavior of the material in the microdomains. Softer microdomains appear brighter than the harder ones.[39] Employed cantilevers were from Nanosensors and had the following characteristics: spring constant of 1.5−6.3 N/m, resonance frequency of 63−100 kHz, tip radius 10 nm. For processing (flattening, filtering) and analysis of AFM images (rms roughness) the program WSxM 4.0 (Develop 7.4) was used. The lateral distances of the microdomains were determined by using the Nanoscope Software ("Modify/2D Spectrum" and "Power Spectral Density Analysis").

Film thicknesses were measured by using the spectroscopic ellipsometer M-2000VI (J.A. Woollam Co. Inc.) with a 50 W QHT lamp as light source. Measurements were made for three angles (65°, 70°, and 75°) in the range between 371 and 1679 nm.

Infrared spectra of the polymer films were recorded with a Bruker IFS 66V/S FTIR spectrometer and a MCT-detector in transition mode. The characteristics of the measurements are as follows: number of scans: 2000; frequency range: 4000−400 cm^{-1}; resolution: 4 cm^{-1}. FT-IR spectra were analyzed with the help of the Bruker software "Opus Version 4.2".

Contact angle measurements were carried out with the goniometer Krüss G40 (Krüss, Hamburg, Germany) applying the sessile drop method. Millipore water was used as liquid.

The in situ synchrotron-SAXS measurements with P(H-OSt-*b*-BOC-OSt) 1:9 (**26**) were carried out at the Polymer Beamline A2 at HASYLAB (DESY Hamburg) in the temperature range between 25 and 250 °C with a heating/cooling rate of 3 K/min. Polymer **26** was employed as powder (as-prepared). In all measurements the wavelength of the X-rays was $\lambda = 0.15$ nm.

Results and Discussion

Choice of Block Copolymers. As mentioned before, partly BOC- and TBU-protected block copolymers on the base of poly(4-hydroxystyrene) offer great potential in terms of hybrid pattering applications, but only when it is possible to control the thin film morphology. Since the volume ratio of the protected and the unprotected block is a crucial point in terms of the formation of a special type of thin film morphology, different block copolymers with varying block ratios have been prepared.[37] The molar masses of the protected and the unprotected poly(4-hydroxystyrene) blocks for the samples used in this study are listed in Table 1 together with their molar mass ratios and the expected morphology of these materials.

The chemical structures of the partly TBU- and BOC-protected block copolymers are depicted in Figure 1.

SAXS Measurements. For the preparation of nanostructured thin films the partly TBU- and BOC-protected block copolymers need to have a sufficient strong tendency to phase-separate into microdomains. As already published recently,[37] the partly TBU-protected block copolymers **19** and **30** are phase-separated in the bulk phase which could be proved by DSC experiments. In the case of the partly BOC-protected block copolymers phase separation could not be shown by that means due to the thermal splitting of the BOC protecting groups at ∼130 °C. Therefore,

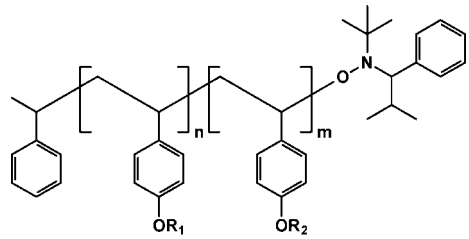

partly protected blockcopolymers:

R_1 = H, R_2 = BOC: 26, 27, 28
R_1 = BOC, R_2 = H: 29

R_1 = TBU, R_2 = H: 19
R_1 = H, R_2 = TBU: 30

Figure 1. General chemical structure of the partly protected block copolymers with the protective groups TBU or BOC.

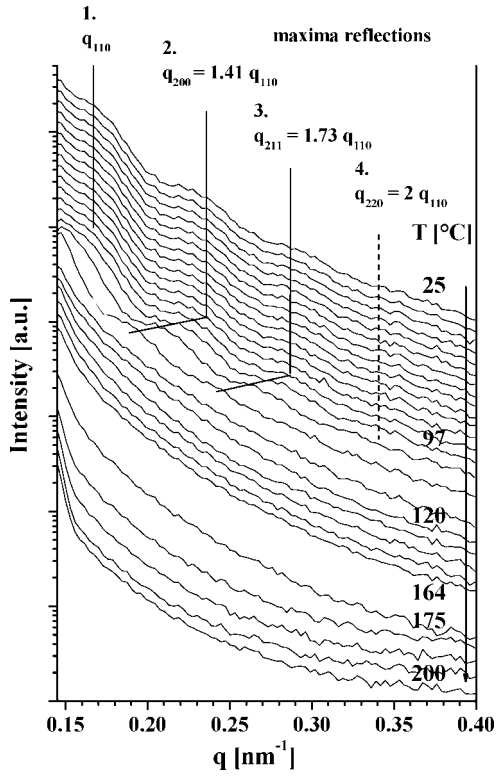

Figure 2. SAXS profiles of P(H-OSt-*b*-BOC-OSt) 1:9 (**26**) at different temperatures. The vertical solid lines show the peak positions of the first, second, and third reflection. The position of the very small fourth reflex maximum is marked with a dashed vertical line. The SAXS curves are shifted for clarity.

SAXS was alternatively favored in order to investigate the phase separation and the microstructure in the bulk phase. P(H-OSt-*b*-BOC-OSt) 1:9 (**26**) was chosen for that study since it has the smallest volume fraction of the unprotected block. If phase separation takes place in **26**, all the other block copolymers P(H-OSt-*b*-BOC-OSt) 1:5 (**27**), 1:3 (**28**), and P(BOC-OSt-*b*-H-OSt) 1:1 (**29**) should also be phase-separated because of their significant higher volume ratios of the unprotected block. The obtained SAXS profiles of a bulk sample of **26** at different temperatures are depicted in Figure 2. In the SAXS curve obtained at room temperature three discrete reflections as well as another very small fourth reflection are recognizable. The first three reflections are relatively plain and broad, so that the isolated maximum can be estimated only with a limited accuracy. However, the SAXS patterns at room temperature clearly indicate that **26** is a phase-separated system. From the relative peak positions of the maxima of the reflections at 1, 1.41, 1.73, and 2 we infer a body-cubic-centered spherical morphology, but the low accuracy of the peaks does not allow to fully proving that phase structure. The spherical microdomains should be composed of the unprotected P(H-OSt) blocks that are located in a matrix of BOC-protected blocks. Upon heating of **26** with a heating rate of 3 K/min, the peak maximum of the corresponding reflections remain at the same position until a temperature of ~97 °C. Above this temperature there is a concerted change of the peaks which corresponds to an expansion of the size of the morphology. This expansion proceeds until about 120 °C; above that, all the reflections disappeared and no nanostructure is discernible. One can easily assume that this process is caused by the increasing miscibility of the different phases above 97 °C, which is also corroborated by the fact that the size of the microstructure is expanded. This process can therefore be considered as an order−disorder transition (ODT). In the temperature range between 120 and 164 °C no significant changes take place. Above 164 °C another process occurs which is indicated by a significant decrease of the scattering intensity. This process can be attributed to the relatively fast thermal removal of the BOC groups. When all BOC groups have been removed, no further processes could be observed at higher temperatures.

Preparation and Characterization of Partly BOC-Protected Block Copolymer Films. As mentioned above, future applications on the basis of nanostructured thin block copolymer films require regular and defined patterns and structures. Since our functional block copolymers have not been studied before with regard to their nanostructure formation in thin films, we had to find appropriate parameters for the thin film preparation and chose, first, the well-established spin-coating technique. Since the bulk morphology of the block copolymer **26** has already been investigated by SAXS, this polymer was also used for film formation in order to compare both systems. The solvent of choice was diglyme because of its ability to dissolve both the BOC-protected and the unprotected block excellently. Additionally, its high boiling point at 162 °C prevents a too rapid evaporation of the solvent during spin-coating procedure, which is not ideal in terms of the formation of regular thin film nanostructures. The microstructure of the as-prepared polymer film was analyzed by TM-AFM measurements, and the obtained results are depicted in Figure 3a.

The phase image depicted in Figure 3a clearly shows a two-phase surface morphology, which consists of a random assembly of dark round-shaped and few elongated microdomains that are embedded in a gray film matrix. In the height image (Supporting Information) one can see that the bright gray film matrix protrudes up to 1 nm over the dark gray microdomains of the unprotected blocks. Nevertheless, the rms roughness of the film is only 0.5 nm so that the film surface can be considered as quite smooth. We assume from the molar mass ratio of the blocks in **26** and also from the morphology in the bulk phase that the dark microdomains consist of the unprotected P(H-OSt) blocks whereas the gray matrix is built up by the BOC-protected blocks. The mean lateral spacing distance of the dark microdomains was determined to be about 30 nm. This is significantly bigger than the thickness of the film, which is ~18 nm as ellipsometric measurements revealed. The observed irregular elongated microdomains which are depicted in both the height and phase images may directly originate from the spin-coating procedure in which the blocks of the polymer have very little time to reach an equilibrium state and to form a more regular pattern.

Other film preparation techniques like dip-coating can circumvent this problem and thus were further explored. The thickness of films prepared by dip-coating strongly depends on

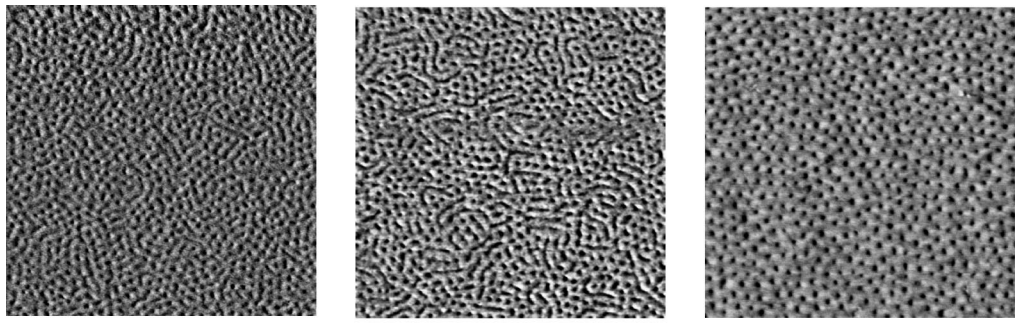

Figure 3. Phase TM-AFM images of an as-deposited polymer film of P(H-OSt-*b*-BOC-OSt) 1:9 (**26**) prepared by (a) spin-coating (3000 rpm, 2 wt % diglyme solution, film thickness 18 nm, lateral scale 1 × 1 μm^2; *z*-gray scale 15°), (b) dip-coating with 11.3 cm/min (1 wt % diglyme solution, film thickness 25 nm, lateral scale 1 × 1 μm^2, *z*-gray scale 6°), and (c) dip-coating with 1.8 cm/min (1 wt % diglyme solution, film thickness 20 nm, lateral scale 0.8 × 0.8 μm^2, *z*-gray scale 6°).

the concentration of the polymer solution and also on the withdrawal rate. Generally, an increase of the withdrawal rate of the substrate leads to thicker polymer films. Varying withdrawal rates can also have a strong impact on the microstructure of the prepared film. In Figure 3b,c the effect of different withdrawal rates on the regularity of the microstructures of polymer films consisting of **26** is illustrated by TM-AFM pictures. For a fast withdrawl rate, apart from the dark round-shaped microdomains, the number of the elongated cylinder-like microdomains is even higher than in the film that was deposited by spin-coating (Figure 3b). Apparently, dip-coating with a relatively fast withdrawal rate of 11.3 cm/min does not lead to a film with a more regular microstructure. In contrast to that, the TM-AFM image in Figure 3c reveals that a slow withdrawal rate gives rise to the formation of a much more regular pattern showing no cylinder-like microdomains. Since the film thicknesses for all samples are similar, one can deduce that the lower solvent evaporation rate during dip-coating with low withdrawal rate gives the block copolymers more time to arrange into a more regular microstructure.

In AFM studies film morphologies are detected up to ~10 nm underneath the film surface.[40,41] This means that by AFM it is not possible to visualize a very thin surface wetting layer of about 2−3 nm on the top of the film but also not the film morphology more than 10 nm below the film surface. Since the film in Figure 3c is 20 nm thick, the entire film morphology cannot be fully revealed by AFM measurements. Because of the fact that the mean lateral distance L_0 of the spherical microdomains is significantly bigger than the film thickness, it is obvious that the film consists of only one layer of the spherical microdomains. These microdomains are surrounded by the film matrix with the BOC-protected blocks. As the film is prepared on a silicon wafer with a polar topmost layer of SiO_2, the formation of a wetting layer with polar P(H-OSt) blocks at the interface between the wafer and the film is energetically favorable. On the other hand, the topmost part of the polymer film can be formed by a thin wetting layer containing only the unpolar BOC-protected blocks which would result in a polymer film with a low surface energy (see for illustration Figure S5 of the Supporting Information).

Contact angle measurements were performed in order to further elucidate the character of the film surface. They revealed an advancing water contact angle of $\theta_a = 89°$ and a receding water contact angle of $\theta_r = 80°$. In a reference experiment with a homopolymer film of P(BOC-OSt) the same values for θ_a and θ_r were obtained. This finding hints to, but does not necessarily prove, a wetting layer on the film since the unpolar polymer matrix of the block copolymer film protrudes up to 1 nm over the more polar round-shaped microdomains which dominates the wetting of the macroscopic water droplet. In Figure 4 a cross-sectional view of the block copolymer film is presented illustrating the topographical situation of the different microdomains.

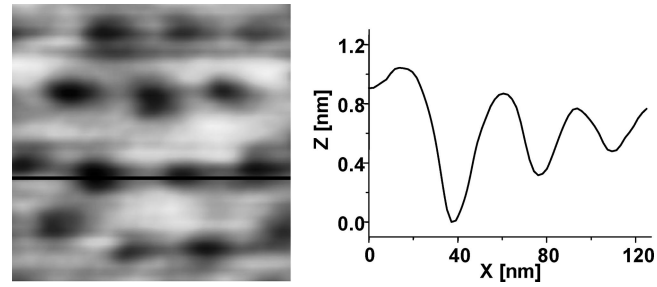

Figure 4. Details (127 nm × 127 nm) of the AFM height image on **26** of the film depicted in Figure 3c together with the corresponding cross section along the black line.

Dip-coating turned out to be also an appropriate method for the preparation of thin nanostructured films with the block copolymers P(H-OSt-*b*-BOC-OSt) 1:5 (**27**) and 1:3 (**28**) as the TM-AFM pictures in Figure 5 show. Best results in terms of a defined nanostructure were obtained when dip-coating was performed with exactly the same solvent (diglyme), concentration (1 wt % polymer solution), and withdrawal rate (1.8 cm/min) as used for the film from **26** depicted in Figure 3c.

Since the molar mass ratio of the BOC-protected block and the unprotected block is 4.7:1 for **27** and 3:1 for **28**, the formation of a cylindrical microstructure in the thin film is expected according to the literature.[2−4] Indeed, the phase images of the films prepared with **27** (Figure 5a) and **28** (Figure 5b) clearly show a fine structure resembling cylindrical, wormlike microdomains. Again, the dark gray wormlike microdomains in Figure 5a,b represent most likely parallel to the substrate aligned cylinders containing the P(H-OSt) blocks which are embedded in a gray film matrix built up by the BOC-protected blocks. Another common feature of the films made of **27** and **28** is that the film matrix with the BOC-protected blocks protrudes about 1 nm over the deeper lying cylinders with the P(H-OSt) blocks. This finding can be seen in analogy to the topographical situation of the polymer films prepared with **26**, which is illustrated in Figure 4. However, an analysis of the surfaces revealed a roughness (rms) of only 0.3 nm for both films so that their overall surfaces are quite smooth.

The different molar masses of the blocks in **27** and **28** have also a direct impact on the mean lateral spacing distance (L_0) of the cylindrical microdomains. Since the molar masses of the unprotected P(H-OSt) blocks are equal in both polymers, L_0 is only increasing with the molar mass of the BOC-protected

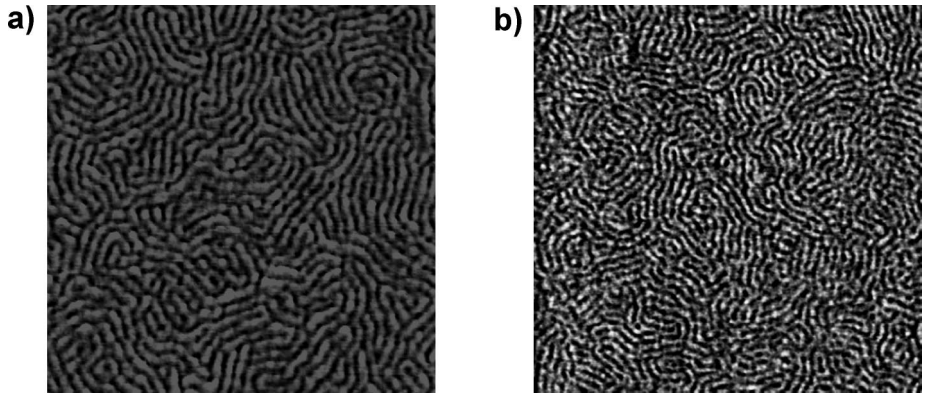

Figure 5. TM-AFM phase images of as-deposited polymer films of P(H-OSt-*b*-BOC-OSt) 1:4.7 (**27**) (a) and P(H-OSt-*b*-BOC-OSt) 1:3 (**28**) (b) prepared by dip-coating (1.8 cm/min, 1 wt % diglyme solution): (a) film thickness 21 nm, *z*-gray scale 18°, 0.9 × 0.9 μm^2; (b) film thickness 19 nm, *z*-gray scale 4°, 1.0 × 1.0 μm^2.

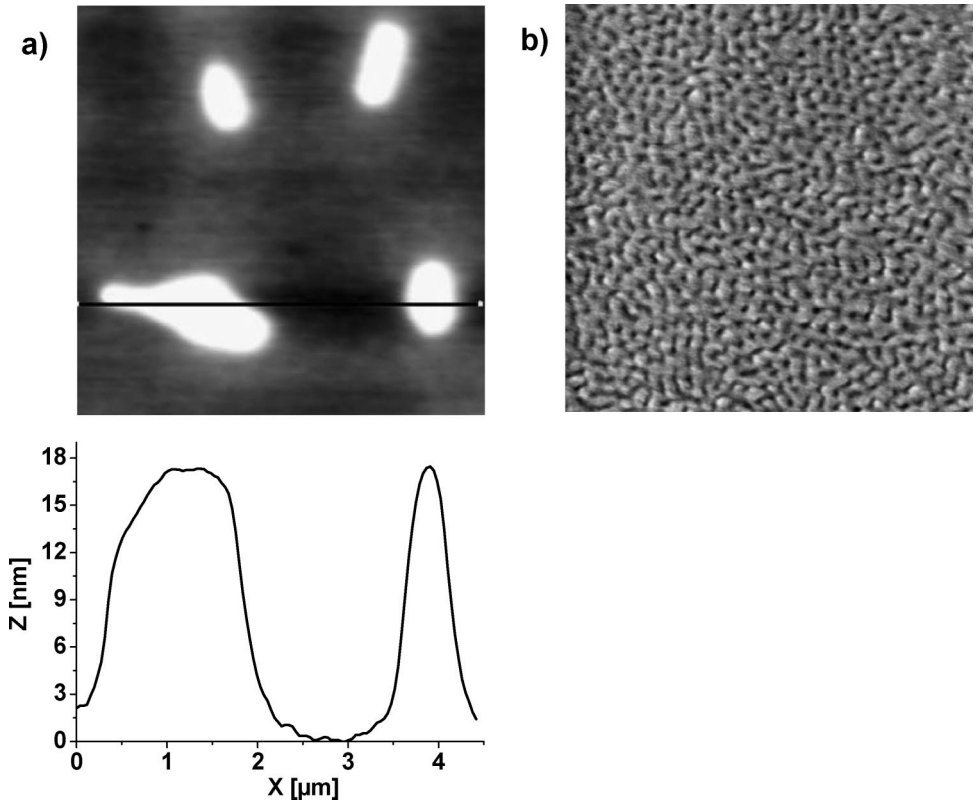

Figure 6. TM-AFM height image (a) with corresponding cross section along the black line and phase image (b) of an as-deposited polymer film of P(BOC-OSt-*b*-H-OSt) 1:1 (**29**) prepared by dip-coating (1.8 cm/min, 1 wt % diglyme solution), film thickness 22 nm: (a) lateral scale 4.5 × 4.5 μm^2, *z*-gray scale 20 nm; (b) lateral scale 1 × 1 μm^2, *z*-gray scale 5°.

blocks. Since $M_{n,cal}$ of the BOC-protected block in **27** is 32 800 g/mol while that of **28** is only 20 700 g/mol, L_0 of the film prepared of polymer **27** (Figure 5a) is with 27 nm significantly larger than that prepared with **28** (Figure 5b), which is only 22 nm. Ellipsometry revealed a film thickness of 21 nm for the film prepared from polymer **27** and 19 nm for the film prepared from **28** so that in both films L_0 is larger than the thickness of the corresponding film.

Unlike the polymers presented above, the block copolymer P(BOC-OSt-*b*-H-OSt) 1:1 (**29**) is nearly symmetrical in terms of the molar masses $M_{n,cal}$ of the unprotected block and the BOC-protected block, which are 14 600 g/mol and 16 100 g/mol, respectively. This should also strongly influence the type of morphology in a thin polymer film. In order to investigate this, a polymer film from **29** was prepared by dip-coating applying the same conditions like for the films discussed above. The topography and the morphology of the as-deposited thin film were analyzed by TM-AFM, and the obtained pictures are depicted in Figure 6.

One can clearly see the formation of islands in the height image (Figure 6a). Because of the symmetric constitution of **29**, the formation of a lamellar morphology is very likely.[2−4] Since the unprotected blocks are very polar, there is a strong affinity of these blocks to concentrate at the interface substrate/film while on the other hand the unpolar BOC-protected blocks should accumulate at the surface of the film in order to lower the surface energy of the film. In the case of such an asymmetric wetting a uniform film thickness is only obtained when the film thickness is $(n + {}^1/_2)L_0$, where n is an integer; otherwise, island, holes, or terraces will be formed.[42] A cross-section analysis of the height image in Figure 6a also shows the height of the islands. It is noteworthy to mention that all islands have nearly

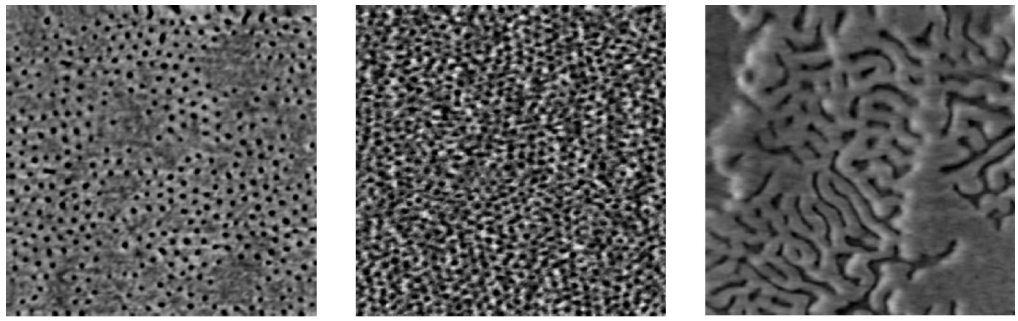

Figure 7. Phase TM-AFM images of an as-deposited polymer film of P(H-OSt-*b*-TBU-OSt) (a) 1:9 (**30**) prepared by dip-coating (1.8 cm/min, 1 wt % diglyme solution), film thickness 16 nm, lateral scale 1 × 1 μm^2, *z*-gray scale 20°; (b) 1:9 (**30**) prepared by dip-coating (1.8 cm/min, 1 wt % dioxane solution), film thickness 18 nm, lateral scale 1 × 1 μm^2, *z*-gray scale 2°; and (c) 1:1 (**19**) prepared by dip-coating (1.8 cm/min, 1 wt % diglyme solution), film thickness 18 nm, lateral scale 1 × 1 μm^2, *z*-gray scale 30°.

the same height of ∼17 nm, and the mean film thickness was 22 nm. Besides this topographic feature, the film reveals also a fine structure at least in some areas of the film as the phase image depicted in Figure 6b shows. However, the shape of the microdomains is not uniform. The existence of such irregular patterns clearly indicates that the film morphology is in a kinetically trapped situation and has not reached its thermodynamic equilibrium.

Preparation and Characterization of Partly TBU-Protected Block Copolymer Films. Similarly as the BOC groups, also the TBU-protecting group can be removed via photoinitiated acidic catalysis; thus, also partly TBU-protected block copolymers are interesting for the concept of hybrid pattering. A thin block copolymer film from P(H-OSt-*b*-TBU-OSt) 1:9 (**30**) was prepared analogously to that of the corresponding partly BOC-protected block copolymer **26** presented in Figure 3c. The recorded TM-AFM phase image is depicted in Figure 7a. Two different types of surface areas are clearly discernible. In one type the film consists of round-shaped microdomains which are embedded in a film matrix. These areas show nearly the same type of microstructure as those which have already been discussed for the corresponding film prepared with the partly BOC-protected block copolymer **26** and depicted in Figure 3c. However, there are also areas where no nanostructure is discernible at all. Interestingly, these areas lay up to 5 nm deeper than the other ones (height images, see Supporting Information). This shows that a change in the film thickness can have a strong impact on the type of the formed nanostructure in a thin block copolymer film.[5−7] As a direct consequence of the varying thicknesses of the different areas, a comparatively high rms roughness of 0.9 nm was observed. The thickness of the film was measured by means of ellipsometry and averages 16 nm.

In order to improve the regularity of the film topography and morphology, dioxane was used instead of diglyme as solvent for the polymer **30**, keeping all other film preparation parameters. Now, a uniform microstructure of dark round-shaped microdomains which are surrounded by a film matrix is observed in the AFM phase image (Figure 7b) which strongly resembles that obtained for the film prepared with polymer **26** (Figure 3c, film thickness 18 nm). In analogy to the morphology discussed for **26**, the dark round-shaped microdomains should represent spheres consisting of the unprotected P(H-OSt) blocks which are embedded in the film matrix constituted by the TBU-protected blocks. As the molar masses of the protected and the unprotected blocks in **26** and **30** are very similar, it is obvious that the mean lateral spacing distance of the spherical microdomains in both films should be nearly the same. Indeed, the analysis of the phase image in Figure 7b showed a L_0 of 31 nm, and the height image (Supporting Information) reveals that the film is very smooth (rms roughness = 0.2 nm). In contrast to **30**, the block copolymer P(H-OSt-*b*-TBU-OSt) 1:1 (**19**) has a very symmetrical composition in terms of the molar masses $M_{n,cal}$ of the TBU-protected and the unprotected blocks which are $M_{n,cal}$ = 23 100 g/mol and $M_{n,cal}$ = 22 800 g/mol, respectively. Similarly as for the BOC-protected sample **29**, this feature has a strong impact on the film topography and morphology (Figure 7c). Highly irregular terrace-like areas with two distinct height levels are discernible in the height images (Supporting Information). The film in the upper bright gray area is ∼7 nm thicker than that in the area of the deeper level contrasted in a darker gray. The phase image in Figure 7c indicates that the topmost layer in both areas most likely consists of the same material since there is no substantial contrast recognizable. We can assume that the microdomains in the film are parallel aligned lamellae forming a superstructure as holes and terrace-like patterns in a similar way as discussed for the corresponding symmetrical partly BOC-protected block copolymer **29**. It is also quite likely that the film morphology is in a kinetically trapped situation and needs a subsequent vapor annealing in order to reach the thermodynamic equilibrium state.

Thermal Switching of the Film Morphology. The BOC groups in the partly BOC-protected block copolymers can be completely thermally decomposed forming the volatile gaseous compounds carbon dioxide and isobutylene.[43] Because of the presence of the slightly acidic phenolic OH groups in the unprotected blocks, the onset temperature of this reaction is already at around 130 °C for our block copolymers, in contrast to that of the homopolymer P(BOC-OSt).[37] At the end of this heating process the block copolymer has been fully transformed into the corresponding homopolymer P(H-OSt). This is accompanied by the loss of the microstructure as the SAXS measurements presented in Figure 2 indicate for the bulk material. In order to demonstrate this process for a thin polymer film, the block copolymer film of **26** presented in Figure 3c was heated at 190 °C for 20 min. As the glass transition temperature of the obtained unprotected P(H-OSt) homopolymer is at around 180 °C,[44] the heating temperature was set at 190 °C to ensure that a flat film can be formed. In Figure 8 the corresponding TM-AFM phase images of the block copolymer film before and after the thermal treatment are presented together with the chemical structures of the polymers. One can clearly see that by the annealing procedure the nanostructured thin film in Figure 8a has been completely transformed into a homogeneous featureless film (Figure 8b). As the rms roughness was determined to be only 0.3 nm, the surface of the annealed film can be considered to be quite smooth. Moreover, the mass loss due to the formation of carbon dioxide and isobutylene leads

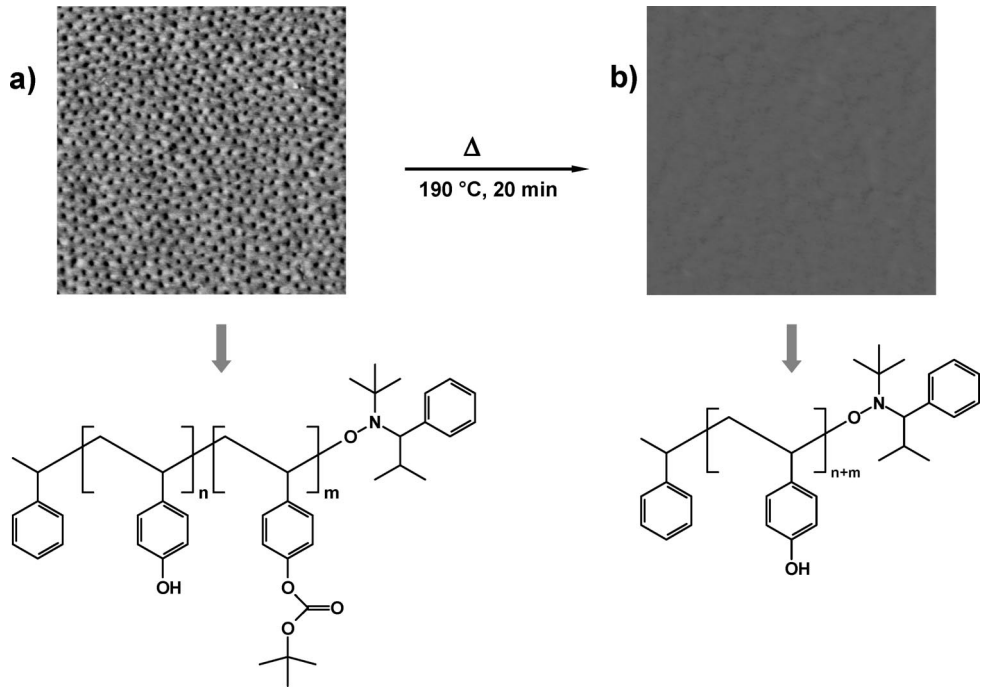

Figure 8. TM-AFM phase images of a polymer film of P(BOC-OSt-*b*-H-OSt) 1:9 (**26**) before (a) and after (b) thermal treatment at 190 °C for 20 min. For (a) details of phase image are given in Figure 3c, thickness 20 nm; (b) film thickness 12 nm, lateral scale 0.6 × 0.6 μm^2, *z*-gray scale 5°.

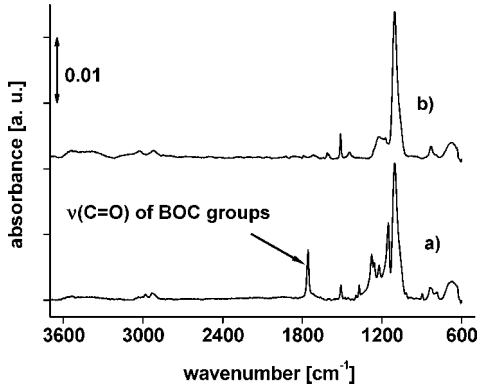

Figure 9. FT-IR spectra of the polymer films of P(BOC-OSt-*b*-H-OSt) 1:9 (**26**) (same as in Figure 8) before (a) and after (b) thermal treatment at 190 °C for 20 min.

also to a significant shrinkage of the film thickness. Ellipsometric measurements reveal that the film thickness decreases from 20 nm before to only 12 nm after the heating procedure. The surface properties of the film like the wettability is also changed which was confirmed by contact angle measurements. The advancing and the receding contact angles of the film decreased from $\theta_a = 89°$ to 69° and from $\theta_r = 80°$ to 41°, respectively. It is also noteworthy to mention that in the literature the value of advancing contact angle for a film of P(H-OSt) was found to be 66°, which is in good agreement with the value of the annealed film.[45]

Despite the fact that the polymer films are very thin, it was possible to detect the removal of the BOC groups by means of FT-IR spectroscopy as the spectra in Figure 9 reveal. The band at $\nu = 1756\ cm^{-1}$ corresponding to the vibration of the carbonyl groups in the BOC groups disappeared after the annealing process, indicating a complete removal of all BOC groups. In order to obtain the genuine spectra of the polymer films, both spectra in Figure 9 were corrected by the FT-IR spectrum of a reference wafer (Si wafer without polymer film).

Conclusions

Partly *tert*-butoxycarbonyl (BOC)- and *tert*-butyl (TBU)-protected block copolymers based on 4-hydroxystyrene with varying block ratios were studied according to their nanostructure in bulk and in thin films. These block copolymers offer the potential for hybrid patterning using the phase segregation on the nanoscale combined with changes in chemical composition on the microscale by the selective deprotection of one block, e.g., through local thermal treatment or photolithography using photoacid generators.

We could show by means of a temperature-dependent SAXS study that the most asymmetric partly BOC-protected block copolymer P(H-OSt-*b*-BOC-OSt) (**26**) with a molar mass ratio of 9 (BOC) to 1 (OH) is in a phase-separated state until the order−disorder transition at ∼120 °C, forming most probably a body-cubic-centered spherical morphology. The thermal removal of the BOC groups at ca. 160 °C groups could also be clearly detected.

Dip-coating with a low withdrawing rate of 1.8 cm/min turned out to be the method of choice for the preparation of as-cast block copolymer films. AFM measurements revealed that the block ratios play a key role in terms of the formation of characteristic morphologies in the thin films. A spherical morphology was found for films prepared of **26**, whereas cylindrical microstructures were formed in those films which were prepared with either the block copolymer P(H-OSt-*b*-BOC-OSt) 1:5 (**27**) or P(H-OSt-*b*-BOC-OSt) 1:3 (**28**). For the nearly symmetrical partly BOC-protected block copolymer P(BOC-OSt-*b*-H-OSt) 1:1 (**29**) very irregular-shaped microdomains were detected, indicating that the film morphology is in a kinetically metastable state.

Annealing of a thin film of **26** at 190 °C resulted in the removal of the BOC groups and thus the transformation of the partly BOC-protected block copolymer into the homopolymer poly(hydroxystyrene) gave rise to a switching of the nanostructured film into a featureless flat homopolymer film which was confirmed by AFM, FT-IR, ellipsometric, and contact angle measurements.

The optimized dip-coating conditions can also be transferred to partly TBU-protected block copolymers samples. The similarity in the film morphology for the partly TBU- and BOC-protected block copolymers of similar composition is a clear indication that the phase behavior is dominated by the poly(4-hydroxystyrene) block, and the chemical interactions within the protected blocks are rather similar for both protecting groups. Thus, with the *p*-hydroxystyrene-based block copolymers a rather robust system was found with the possibility to prepare over a broad composition range reproducible and well-ordered nanostructures in thin films. This allows also to fine-tune the nanostructure features and sizes by the block copolymer characteristics. By combining blocks with TBU- and BOC-protected groups, it might even be possible to have a two-step change in nanostructure, from homogeneous (TBU/BOC hydroxystyrene-based block copolymer), to phase-separated (TBU-HO-St block copolymer), to homogeneous (HO-St homopolymer), making use of the different option regarding removal of the protecting groups.

In future studies, the long-range order of the nanostructured block copolymer films as well as the hybrid patterning concept will be investigated. This will be the base for the potential use of our block copolymers in a bottom-up approach for the preparation of nanoscopic devices. The possibility to combine the proven nanostructure formation in thin films by the phase separation process with classical lithographic methods renders our materials highly interesting for that application.

Acknowledgment. The authors thank Ms. G. Adam for performance of the FT-IR measurements, Ms. S. Reichelt and Dr. Y. Mikhaylova for ellipsometric measurements, Dr. S. Funari at DESY (Hamburg) for facilitating SAXS investigations, and Dr. I. Tokarev and Dr. A. Sidorenko for advice concerning film preparation by dip-coating. Mr. A. Janke is thanked for assistance and interpretation related to TM-AFM studies. Financial support from the Deutsche Forschungsgemeinschaft (DFG) in the frame of the Collaborative Research Center 287 is also gratefully acknowledged.

Supporting Information Available: Full pairs of height and phase AFM images. This material is available free of charge via the Internet at http://pubs.acs.org.

References and Notes

(1) Lazzari, M.; Lopez-Quintela, M. A. *Adv. Mater.* **2003**, *15*, 1583–1594.
(2) Förster, S.; Plantenberg, T. *Angew. Chem.* **2002**, *114*, 712–739.
(3) Bates, F. S.; Fredrickson, G. H. *Annu. Rev. Phys. Chem.* **1990**, *41*, 525–557.
(4) Bates, F. S. *Science* **1991**, *251*, 898–905.
(5) Knoll, A.; Horvat, A.; Lyakova, K. S.; Krausch, G.; Sevink, G. J. A.; Zvelindovsky, A. V.; Magerle, R. *Phys. Rev. Lett.* **2002**, *89*, 035–501.
(6) Krausch, G.; Magerle, R. *Adv. Mater.* **2002**, *14*, 1579–1583.
(7) Fasolka, M. J.; Banerjee, P.; Mayes, A. M.; Pickett, G.; Balazs, A. C. *Macromolecules* **2000**, *33*, 5702–5712.
(8) Morkved, T. L.; Lu, M.; Urbas, A. M.; Ehrichs, E. E.; Jaeger, H. M.; Mansky, P.; Russell, T. P. *Science* **1996**, *273*, 931–933.
(9) Thurn-Albrecht, T.; Schotter, J.; Kästle, G. A.; Emley, N.; Shibauchi, T.; Krusin-Elbaum, L.; Guarini, K.; Black, C. T.; Tuominen, M. T.; Russell, T. P. *Science* **2000**, *290*, 2126–2129.
(10) Thurn-Albrecht, T.; DeRouchey, J.; Russell, T. P.; Jaeger, H. M. *Macromolecules* **2000**, *33*, 3250–3253.
(11) Thurn-Albrecht, T.; DeRouchey, J.; Russell, T. P.; Kolb, R. *Macromolecules* **2002**, *35*, 8106–8110.
(12) Huang, E.; Rockford, L.; Russell, T. P.; Hawker, C. J. *Nature (London)* **1998**, *395*, 757–758.
(13) Mansky, P.; Liu, Y.; Huang, E.; Russell, T. P.; Hawker, C. *Science* **1997**, *275*, 1458–1460.
(14) Kim, G.; Libera, M. *Macromolecules* **1998**, *31*, 2569–2577.
(15) Lin, Z.; Kim, D. H.; Wu, X.; Boosahda, L.; Stone, D.; LaRose, L.; Russell, T. P. *Adv. Mater.* **2002**, *14*, 1373–1376.
(16) Temple, K.; Kulbaba, K.; Power-Billard, K. N.; Manners, I.; Leach, A.; Xu, T.; Russell, T. P.; Hawker, C. J. *Adv. Mater.* **2003**, *15*, 297–300.
(17) Kim, S. H.; Misner, M. J.; Xu, T.; Kimura, M.; Russell, T. P. *Adv. Mater.* **2004**, *16*, 226–231.
(18) Kim, S. H.; Misner, M. J.; Russell, T. P. *Adv. Mater.* **2004**, *16*, 2119–2123.
(19) Cheng, J. Y.; Ross, C. A.; Thomas, E. L.; Smith, H. I.; Vancso, G. J. *Appl. Phys. Lett.* **2002**, *81*, 3657–3659.
(20) Cheng, J. Y.; Ross, C. A.; Thomas, E. L.; Smith, H. I.; Vancso, G. J. *Adv. Mater.* **2003**, *15*, 1599–1602.
(21) Cheng, J. Y.; Zhang, F.; Smith, H. I.; Vancso, G. J.; Ross, C. A. *Adv. Mater.* **2006**, *18*, 597–601.
(22) Ruiz, R.; Sandstrom, R. L.; Black, C. T. *Adv. Mater.* **2007**, *19*, 587–591.
(23) Park, S.-M.; Stoykovich, M. P.; Ruiz, R.; Zhang, Y.; Black, C. T.; Nealey, P. F. *Adv. Mater.* **2007**, *19*, 607–611.
(24) Ruiz, R.; Ruiz, N.; Zhang, Y.; Sandstrom, R. L.; Black, C. T. *Adv. Mater.* **2007**, *19*, 2157–2162.
(25) Cheng, J. Y.; Ross, C. A.; Smith, H. I.; Thomas, E. L. *Adv. Mater.* **2006**, *18*, 2505–2521.
(26) Kim, S. O.; Solak, H. H.; Stoykovich, M. P.; Ferrier, N. J.; de Pablo, J. J.; Nealey, P. F. *Nature (London)* **2003**, *424*, 411–414.
(27) Edwards, E. W.; Stoykovich, M. P.; Müller, M.; Solak, H. H.; de Pablo, J. J.; Nealey, P. F. *J. Polym. Sci., Part B: Polym. Phys.* **2005**, *43*, 3444–3459.
(28) Kim, S. O.; Kim, B. H.; Meng, D.; Shin, D. O.; Koo, C. M.; Solak, H. H.; Wang, Q. *Adv. Mater.* **2007**, *19*, 3271–3275.
(29) Park, S.-M.; Craig, G. S. W.; La, Y.-H.; Solak, H. H.; Nealey, P. F. *Macromolecules* **2007**, *40*, 5084–5094.
(30) Thurn-Albrecht, T.; Steiner, R.; DeRouchey, J.; Stafford, C. M.; Huang, E.; Bal, M.; Tuominen, M.; Hawker, C. J.; Russell, T. P. *Adv. Mater.* **2000**, *12*, 787–790.
(31) Russell, T. P.; Thurn-Albrecht, T.; Tuominen, M.; Huang, E.; Hawker, C. J. *Macromol. Symp.* **2000**, *159*, 77–88.
(32) Du, P.; Li, M.; Douki, K.; Li, X.; Garcia, C. B. W.; Jain, A.; Smilgies, D.-M.; Fetters, S. J.; Gruner, S. M.; Wiesner, U.; Ober, C. K. *Adv. Mater.* **2004**, *16*, 953–957.
(33) Reichmanis, E.; Thompson, L. F. *Chem. Rev.* **1989**, *89*, 1273–1289.
(34) Reichmanis, E.; Houlihan, F. M.; Nalamasu, O.; Neenan, T. X. *Chem. Mater.* **1991**, *3*, 394–407.
(35) MacDonald, S. A.; Willson, C. G.; Fréchet, J. M. J. *Acc. Chem. Res.* **1994**, *27*, 151–158.
(36) Fréchet, J. M. J.; Kallman, N.; Kryczka, B.; Eichler, E.; Houlihan, F. M.; Willson, C. G. *Polym. Bull.* **1998**, *20*, 427–434.
(37) Messerschmidt, M.; Millaruelo, M.; Komber, H.; Häuβler, L.; Voit, B.; Krause, T.; Yin, M.; Habicher, W.-D. *Macromolecules* **2008**, *41*, 2821–2831.
(38) Tokarev, I. Ph.D. Thesis, Technical University of Dresden, **2004**.
(39) Magonov, S. N.; Elings, V.; Whangbo, M.-H. *Surf. Sci.* **1997**, *375*, L385−L391.
(40) Knoll, A.; Magerle, R.; Krausch, G. *Macromolecules* **2001**, *34*, 4159–4165.
(41) Knoll, A. Ph.D. Thesis, University of Bayreuth, **2003**.
(42) Kellogg, G. J.; Walton, D. G.; Mayes, A. M.; Lambooy, P.; Russell, T. P.; Gallagher, P. D.; Satija, S. K. *Phys. Rev. Lett.* **1996**, *76*, 2503–2506.
(43) Fréchet, J. M. J.; Eichler, E.; Ito, H.; Willson, C. G. *Polymer* **1983**, *24*, 995–1000.
(44) Barclay, G. G.; Hawker, C. J.; Ito, H.; Orellana, A.; Malenfant, P. R. L.; Sinta, R. F. *Macromolecules* **1998**, *31*, 1024–1031.
(45) Augsburg, A.; Grundke, K.; Pöschel, K.; Jacobasch, H.-J.; Neumann, A. W. *Acta Polym.* **1998**, *49*, 417–426.

MA8019915